IOP PUBLISHING PLASMA PHYSICS AND CONTROLLED FUSION

Plasma Phys. Control. Fusion **49** (2007) A29–A44 doi:10.1088/0741-3335/49/5A/S03

Multi-machine studies of the role of turbulence and electric fields in the establishment of improved confinement in tokamak plasmas

G Van Oost[1], V V Bulanin[2], A J H Donné[3], E Z Gusakov[4], A Kraemer-Flecken[5], L I Krupnik[6], A Melnikov[7], S Nanobashvili[8], P Peleman[1], K A Razumova[7], J Stöckel[9] ,V Vershkov[7], J Adamek[9], A B Altukov[4], V F Andreev[7], L G Askinazi[4], I S Bondarenko[6], J Brotankova[9], A Yu Dnestrovskij[7], I Duran[9], L G Eliseev[7], L A Esipov[4], S A Grashin[7], A D Gurchenko[4], G M D Hogeweij[3], M Hron[9], C Ionita[10], S Jachmich[11], S M Khrebtov[6], D V Kouprienko[4], S E Lysenko[7], E Martines[12], S V Perfilov[7], A V Petrov[2], A Yu Popov[4], D Reiser[5], R Schrittwieser[10], S Soldatov[5], M Spolaore[12], A Yu Stepanov[4], G Telesca[1], A O Urazbaev[7], G Verdoolaege[1], F Zacek[9] and O Zimmermann[5]

[1] Department of Applied Physics, Ghent University, Ghent, Belgium
[2] St Petersburg State Polytechnical University, St Petersburg, Russia
[3] FOM-Institute for Plasma Physics Rijnhuizen, Association EURATOM-FOM, Nieuwegein, The Netherlands
[4] Ioffe Institute, 194021, St Petersburg, Russia
[5] Institute of Plasma Physics, Forschungszentrum Jülich GmbH, EURATOM Association, Jülich, Germany
[6] Institute of Plasma Physics, NSC 'Kharkov Institute of Physics and Technology', Kharkov, Ukraine
[7] Nuclear Fusion Institute, RRC, 'Kurchatov Institute', 123182 Moscow, Russian Federation
[8] Andronikashvili Institute of Physics, Tbilisi, Georgia
[9] Institute of Plasma Physics, Association EURATOM/IPP.CR, Prague, Czech Republic
[10] Department of Ion Physics, University of Innsbruck, Innsbruck, Austria
[11] Laboratory for Plasma Physics, ERM/KMS,Association EURATOM-Belgian State Brussels, Belgium
[12] Consorzio RFX, Associazione EURATOM-ENEA sulla Fusione, Padova, Italy

E-mail: Guido.VanOost@UGent.be

Received 21 July 2006, in final form 11 October 2006
Published 27 March 2007
Online at stacks.iop.org/PPCF/49/A29

Abstract

An extensive (INTAS) research programme started in 2002 to investigate the correlations between, on the one hand, the occurrence of transport barriers and improved confinement in the medium-size tokamaks TEXTOR and T-10 and on the smaller tokamaks FT-2, TUMAN-3M and CASTOR, and on the other hand, electric fields, modified magnetic shear and electrostatic and magnetic turbulence using advanced diagnostics with high spatial and temporal resolution, and various active means to externally control plasma transport. It also requires one to characterize fluctuations of various important plasma

parameters inside and outside transport barriers (TBs) and pedestal regions with high spatial and temporal resolution using advanced diagnostics, and to elucidate the role of turbulence driving and damping mechanisms, including the role of the plasma edge properties. Furthermore, one needs to determine the cross-field transport from the measurements and compare this with available theoretical models. This has been done in a strongly coordinated way, exploiting the complementarity of TEXTOR and T-10 and the backup potential of the three other tokamaks, which together have all the relevant experimental tools and theoretical expertise. Physical mechanisms of several TBs have been studied: electron internal transport barriers in T-10 and TEXTOR, ergodization-induced TB in TEXTOR, TB in ohmic discharges in TUMAN-3M, periodic bias-induced TBs in CASTOR. Geodesic acoustic modes (GAM) have been investigated in T-10, TEXTOR and TUMAN-3M. Core turbulence has been characterized in T-10, and small-scale turbulence has been revealed in FT-2.

(Some figures in this article are in colour only in the electronic version)

1. Introduction

The understanding and reduction of turbulent transport in magnetic confinement devices is not only an academic task but also a matter of practical interest, since high confinement has been chosen as the regime for ITER and possible future reactors because it reduces size and cost. Generally speaking, turbulence comes in two classes: electrostatic and magnetic turbulence. Over the past decade, step-by-step new regimes of plasma operation have been identified, whereby turbulence can be externally controlled, which led to better and better confinement. About a decade ago local zones (called internal transport barriers, ITBs) with reduced transport were discovered in tokamaks. These ITBs can act on the electron and/or ion fluid.

The physical picture that is generally given is that by spinning up the plasma, it is possible to create flow velocity shear large enough to tear turbulent eddies apart before they can grow, thus reducing electrostatic turbulence. This turbulence stabilization concept has the universality, needed to explain *ion transport* barriers at different radii seen in limiter and divertor tokamaks, stellarators, reversed field pinches, mirror machines and linear devices with a variety of discharge- and heating conditions and edge biasing schemes.

The *electron heat conduction*, however, which normally is 1–2 orders above the collisional lower limit, remained strongly anomalous also in the regime with suppressed electrostatic turbulence. In that case it became the dominant heat loss channel. From this, it is conjectured that magnetic turbulence drives the anomalous electron heat conduction. Experiments at the T-10 tokamak which specifically addressed the electron thermal transport properties of the plasma have strongly corroborated this conjecture (see section 3.1) and demonstrated that flow velocity shear is not the reason for confinement increase in the electron ITB region, but most likely a consequence of ITB formation. It was shown that e-ITBs form when contact between turbulent cells located at rational surfaces is broken. This may be seen at low number rational surfaces ($m/n = 1/1, 2/1, 3/2$ and so on).

Although turbulence measurements have been performed on many magnetic confinement devices during the past decade, the additional insight gained from these experiments is relatively limited. This can be attributed to a number of reasons:

- Firstly, only a very coarse spatial resolution was achieved in many measurements of electric fields and turbulence.

- Secondly, simultaneous measurements of different fluctuating quantities (temperature, density, electric potential and magnetic field) at the same location, needed for a quantitative estimation of the energy and particle transport due to turbulence were only performed in a very limited number of cases.
- Thirdly, theoretical models were often only predicting the global level of turbulence as well as the scaling of this level with varying plasma parameters.

The investigation of the correlations between, on the one hand, the occurrence of transport barriers and improved confinement in magnetically confined plasmas, and on the other hand, electric fields, modified magnetic shear and electrostatic and magnetic turbulent fluctuations necessitates the use of various active means to externally control plasma transport. It also requires one to characterize fluctuations of various important plasma parameters inside and outside transport barriers and pedestal regions with high spatial and temporal resolution using advanced diagnostics, and to elucidate the role of turbulence driving and damping mechanisms, including the role of the plasma edge properties. The experimental findings have to be compared with advanced theoretical models and numerical simulations.

The Consortium of the INTAS project 2001-2056 disposes of five tokamaks (the medium-size and similar tokamaks TEXTOR and T-10, and the smaller-scale tokamaks FT-2, TUMAN-3M and CASTOR), equipped with advanced diagnostics with high spatial and temporal resolution. Research activities are strongly coordinated and exploit the complementarity of TEXTOR (mainly ion heating, dynamic ergodic divertor (DED)) and T-10 (electron heating, heavy ion beam probe (HIBP)) as well as the backup potential of the three other tokamaks, which together have all the relevant experimental tools and theoretical expertise.

Improvement and development of diagnostics which were necessary for the successful execution of the project are briefly outlined in section 2. The most important results obtained in the investigations of the physical mechanisms underlying different types of transport barriers are presented in section 3. The results of studies on turbulence characteristics are discussed in section 4.

2. Improvement and development of diagnostics

2.1. Heavy ion beam probe (HIBP)

The HIBP is the only diagnostic which is able to measure the plasma electric potential and its fluctuations in the bulk plasma [1]. The spontaneous changes of the edge plasma potential during L-H transition have been measured by HIBP in tokamaks, but the steady-state edge profiles have not been reported so frequently. To probe the plasma core in the T-10 tokamak ($R_0 = 1.50$ m, $a = 0.30$ m) [2], Tl^+ ions were accelerated up to 240 kV. The recent modification of the beam lines and the entrance ports expands the HIBP observation area in the upper outer quadrant of the plasma cross section. The plasma was limited by the movable rail limiter at $a_{\rm lim} = 0.27$–0.3 m and the circular limiter at $a_{\rm clim} = 0.33$ m. HIBP was able to operate in the range of normalized radius $0.57 < \rho < 1.0$ (depending on $B_{\rm t}$), providing the plasma potential profile along with the probing beam current $I_{\rm tot}$ which represents the density profile. The observed radial interval moves towards the plasma centre with decreasing $B_{\rm t}$. The sample volume position in the plasma in a single discharge can be either fixed or scanned radially with a period of 10 ms, producing a series of profiles during a single shot. Sample volumes look like elliptical discs, approximately 1 cm × 1.5 cm (radial) × 0.5 cm (thickness). The uncertainty in the sample volume position was up to 2 cm. Correlation reflectometry (CR) was able to

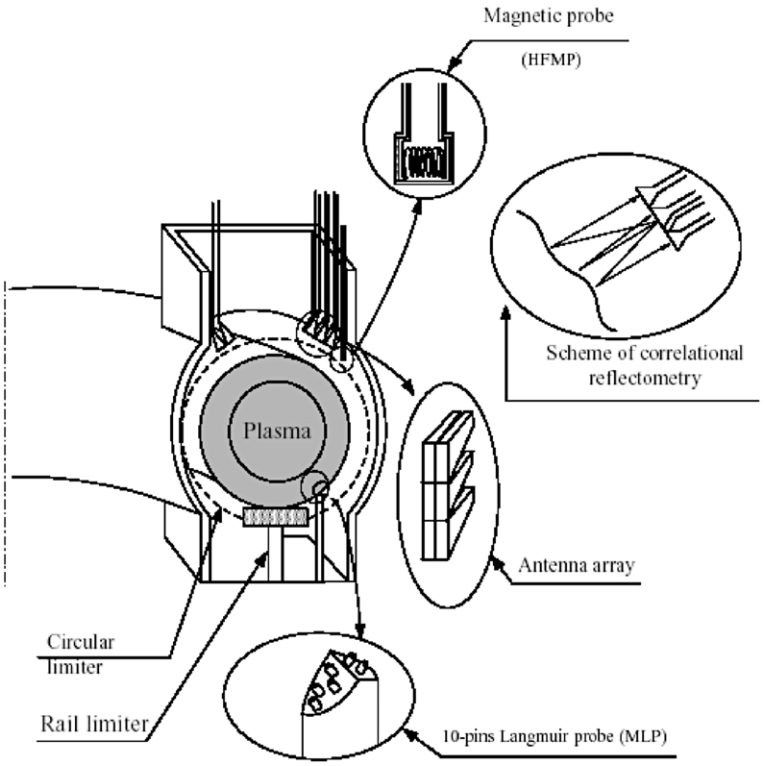

Figure 1. Schematics of correlation reflectometer, high frequency magnetic probe and multipin Langmuir probe diagnostics and limiters on the T-10 tokamak.

observe the whole plasma. At the plasma edge ($0.95 < \rho < 1.2$) they both overlapped with Langmuir probes.

2.2. Correlation reflectometry (CR)

The CR system on T-10 [3] had two antenna arrays, probing the plasma from the low field side (LFS) and the high field side (HFS). As shown in figure 1, both the arrays were located at the top of the plasma column shifted at $\approx 30^{\circ}$ to both sides with respect to the vertical central line. All antennas were mounted at radius 41 cm and aligned to the centre of the vacuum vessel. The LFS array had six pyramidal horns with width 2.5 cm, height 4 cm and length 12 cm. The HFS array had two horns with similar dimensions. It was possible to probe the plasma simultaneously from both the HFS and the LFS in order to measure the poloidal asymmetry of the turbulence and long-distance poloidal and toroidal correlations. The reflection of the O-mode with electric field vector of the launched wave parallel to the magnetic field was used. The frequency range varied from 22 to 78 GHz corresponding to the densities in the reflection point ranging from 0.6×10^{19} to 7.5×10^{19} m^{-3}, enabling measurements over the whole plasma radius.

Previously the three-wave heterodyne reflectometer was used, where two sideband satellites were produced in addition to the launching frequency by means of amplitude

modulation with p-i-n diode. The sampling rate of the ADCs (analog-to-digital converters) was 1 MHz. Although such a system has the intrinsic capability to measure the radial correlations in each discharge, it was replaced by four independent heterodyne reflectometers, covering the full frequency range. Their local oscillators had a phase lock loop in order to hold intermediate frequency (IF) at 20 MHz. This was done to measure correlations at large radial separations and long-distance toroidal correlations. The use of a heterodyne system ensures high sensitivity of reflectometers. Up to three reflectometers have been used in a single discharge, providing a wide range of poloidal and radial correlation measurements.

An O-mode poloidal CR system [4] has been installed at TEXTOR ($R_0 = 1.75$ m, $a = 0.47$ m) [5]. Its relatively low frequency (LF) range between 26 and 37 GHz is adjusted along the requirements of the DED operation in plasmas with medium electron density. The reflectometer can be operated with two antenna arrays, one in the equatorial plane and the other at the top of the vessel which each consist of five pyramidal horn antenna. Both arrays are installed in the same poloidal cross section. The simultaneous measurement of toroidal, poloidal and turbulence velocity makes the comparison between plasma and turbulence velocity possible. For different radii and different toroidal plasma rotations in co- and counter-current directions, both, the LF and the quasi-coherent (QC) modes are frozen in the plasma. Within the accuracy of the measurements, an additional phase velocity of the turbulence, with respect to the plasma velocity, can be neglected. This offers the possibility to derive the radial electric field from the measurement of the turbulence rotation.

2.3. Doppler reflectometry

Microwave Doppler reflectometry is now extensively employed as an effective tool for plasma rotation measurements in toroidal devices. The method is based on the derivation of the rotation velocity from the Doppler frequency shift of backscattered radiation expected under an oblique incidence of the microwave beam onto the cut-off surface. Fair radial resolution of the diagnostics is obtained due to microwave field enhancement in the vicinity of the cut-off. The 2D simulations of the Doppler reflectometry showed that the resolution of the method proposed worsens with increasing curvature of the cut-off surface. Conditions were determined under which the resolution of the diagnostics in small- and medium-size tokamaks can be substantially improved by using converging microwave beams. The approach developed for the simulation has been used for modelling of Doppler reflectometry experiments in the TUMAN-3M tokamak ($R_0 = 0.53$ m, $a = 0.25$ m) [6].

2.4. Correlative enhanced scattering diagnostic

The giant Doppler frequency shift effect of the highly localized microwave backscattering (BS) in the upper hybrid resonance (UHR) has been investigated in detail and applied as plasma rotation diagnostic at the FT-2 tokamak ($R_0 = 0.55$ m, $a = 0.08$ m), where a steerable focusing antenna set, allowing off-equatorial plane plasma X-mode probing from the high magnetic field side, is installed [7]. A separate line less than 1.5 MHz wide and shifted by up to 2 MHz is routinely observed in the BS spectrum under the condition of accessible UHR. The line frequency shift is proportional to the antenna vertical displacement and dependent on the UHR position, changing sign in the vicinity of the last closed flux surface (LCFS). The line width is proportional to its shift. The enhancement of the Doppler frequency shift is explained by the growth of the poloidal wave number of the probing wave in the UHR, typical for toroidal machines. This new diagnostic scheme for the local measurement of plasma poloidal rotation has been benchmarked against Doppler reflectometry data and applied to detailed local study

of plasma poloidal rotation profiles in FT-2 ohmic discharges at different plasma densities and current.

2.5. Fluctuation reflectometry analytical theory

Spatial and wave number resolution of Doppler, radial correlation and poloidal correlation microwave reflectometry techniques have been studied in realistic 2D geometry for arbitrary density and turbulence profiles accounting for diffraction and refraction effects and curvature of magnetic surfaces [8, 9]. The important role of poor localized small angle scattering in the formation of the fluctuation reflectometry signal is demonstrated. The criteria describing transition of diagnostics into nonlinear multiple small angle scattering regime are established. A simple looking expression allowing reconstruction of turbulence profile based on the fluctuation reflectometry data, obtained in linear regime, is given. The possibility of obtaining plasma rotation and turbulence characteristics even in nonlinear regime of radial correlation and Doppler reflectometry is shown.

2.6. Novel advanced Gundestrup-like probe

A novel advanced Gundestrup-like probe head for local measurements of equilibrium and fluctuating plasma parameters in the plasma edge of TEXTOR has been developed [10]. This probe assembly enables us to simultaneously determine the toroidal and poloidal plasma flow, the ion saturation current, density, electron temperature, floating potential as well as their fluctuating properties. An improved analytical probe model is used to correctly relate the ratio of the ion saturation currents measured at the upstream and downstream collecting surfaces to the plasma flow. The probe is mounted on a fast reciprocating manipulator resulting in a high radial resolution of the profiles. A unique feature of the fast probe is the electrical linear motor drive which allows predefining any waveform of the radial position. The high speed of the probe drive reduces the exposure time, which enables us to measure several radial profiles within a single discharge deep inside the LCFS.

3. Transport barriers: physical mechanisms

3.1. Electron internal transport barriers

Recent research in the T-10 and TEXTOR devices has concentrated on understanding the physical mechanisms that are responsible for the generation of electron internal transport barriers (e-ITBs) and also on finding out in which way they are related to the concept of profile consistency, in which the plasma pressure and temperature profiles have a tendency to organize themselves [11, 12] into a 'universal' profile shape, in agreement with the plasma minimum free energy principle. If ∇p exceeds a certain critical value, instabilities connected with the pressure gradient will counteract the formation of an even steeper gradient. The radial distribution of transport coefficients is determined by the necessity to maintain the self-consistent pressure profile under different external impacts.

Previous work [13] has shown that e-ITBs are formed when $\mathrm{d}q/\mathrm{d}r$ is low in the vicinity of rational magnetic surface with low m and n values. The investigation of effects bound with ITB formation was continued in T-10 experiments in 2005. For this purpose experiments with a rapid plasma current ramp up were performed. In this case, due to $(\beta_\mathrm{p} + l_\mathrm{i}/2) \sim 1/I_\mathrm{p}^2$ a rapid change of the magnetic surface densities in the central part of plasma takes place, while current penetration in this region occurs only after $t > 50$ ms. So confinement changes observed in the plasma core are the result of a magnetic surface density change only [14].

Experiments have been conducted on T-10 to investigate the interplay between the formation of e-ITB and the maintenance of self-consistent plasma profiles under the action of electron cyclotron resonance heating and current drive ECRH/ECCD. A joint analysis of T-10 and TEXTOR experimental results enabled to analyse effects bound with plasma self-organization. It was shown that the plasma pressure profiles obtained in different operational regimes and even in various tokamaks may be represented by a single typical curve, called the self-consistent pressure or canonical profile, also often referred to as profile resilience or profile stiffness [12].

The investigation of self-consistent pressure profile effects was carried out under different experimental conditions, such as regimes with plasma density near the Greenwald limit and regimes with deuterium pellet injection. It can be concluded that the effect takes place in a wide region of plasma density up to that, which leads to disruption. The conditions described by this self-consistent profile are realized in a very short time, less than the experimental time resolution $\Delta t \geqslant 2$–4 ms. During ECRH it is realized by a plasma density redistribution: n_e decreases in the plasma heating zone. This implies that the famous 'density pump out' is the result of plasma self-consistent organization. Experimentally this means that, when one tries to distort the self-consistent pressure profile, the heat (cold) pulse spreads much more quickly than can be expected from transport coefficients, calculated from a radial power balance. Since the self consistency effect is exactly valid for the plasma pressure profile we suggest the hypothesis that it is determined by the density of the turbulent cells, which have to be located at rational surfaces. The pressure gradient changes the distance between such cells and hence the turbulent flux. However, in ITB regions ∇p can largely exceed that of the self-consistent pressure profile. The question whether our hypothesis can explain external TB formation problem needs more investigations, partly on smaller tokamaks.

The T-10 results, as well as recent results from JET [15] and DIII-D [16] show that ITBs are formed in the vicinity of low-order rational surfaces, where the gap between rational surfaces is large. The ITB formation is the result of the regulation of turbulent flux by changing the contact between the turbulent cells. It seems that so-called 'hybrid' regimes can also be explained by such hypothesis: magnetic shear close to zero leads to more rarified rational surfaces, especially, when they are located near a low-order rational surface. Nevertheless, the plasma confinement has to depend on the width of the turbulent cells and its dependence on plasma parameters. Rational surfaces play a key role in the establishment of ITBs, as has been observed in stellarators, too [17]. However, this does not exclude a possible supporting role of ExB shear in ITB formation near rational surfaces (interaction between neighbouring cells). Recent work on DIII-D and gyrokinetic simulations [16] hint at possible synergy between ExB shear and effects of rational surfaces. Large profile corrugations in electron temperature gradients (ETGs) at lowest-order singular surfaces lead to the build-up of a huge zonal flow ExB shear layer which provides a trigger for the low power ITB observed in DIII-D.

3.2. Transport barriers induced by dynamic ergodic divertor (DED) in TEXTOR

The influence of a magnetic perturbation field, generated by the DED, on the turbulence and transport properties is studied and compared with plasmas without such a field perturbation. The external magnetic field breaks up the magnetic field lines structure and causes an ergodization of the plasma edge [18]. The strength and radial range of the perturbation field can be widely varied. The influence of DED combined with tangential neutral beam injection in co- and counter-current directions, on turbulent transport has been investigated.

One main effect of the DED is the modification of the radial electric field. The ergodization of the magnetic field lines leads to an increased electron loss rate which charges the plasma

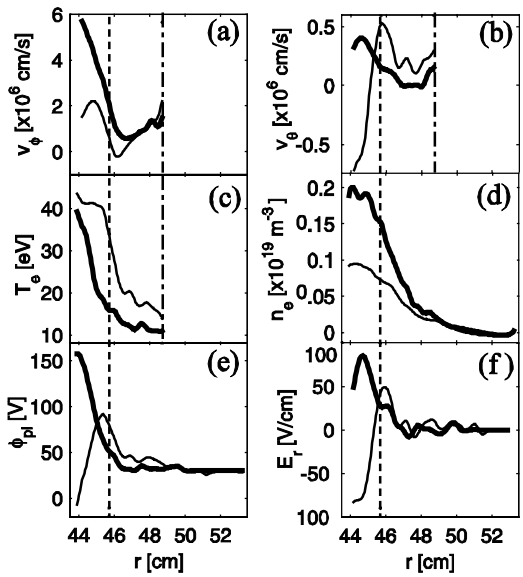

Figure 2. Radial profiles (#99777) of the (*a*) toroidal flow v_ϕ, (*b*) poloidal flow v_θ, (*c*) electron temperature T_e, (*d*) electron density n_e, (*e*) floating potential ϕ_f and, (*f*) radial electric field E_r before (——) and during (——) DED in TEXTOR. The vertical dashed line marks the position of the LCFS. The dashed-dotted line indicates the end of the reliability of the Gundestrup data.

edge more positively. The application of the DED increases the rotation in the scrape-off-layer, where the original rotation is in the ion diamagnetic drift direction. Since the rotation at radii smaller than the limiter radius is in the electron diamagnetic drift direction, the DED slows down the rotation. The inversion point of the radial electric field (as well as the poloidal rotation velocity) is shifted further inside. This effect does not depend on the DED configuration ($m/n = 3/1$ or $12/4$), but on the field strength of the perturbation field. Note that this conclusion concerns only DC DED operation; the AC DED scenarios are the subject of future work.

The data obtained in a single discharge with the fast scanning Gundestrup probe (figure 2) clearly demonstrate the effects of DED on the plasma edge parameters [19].

The combination of counter-current neutral beam injection and the DED can lead to the formation of a transport barrier at the plasma edge [20]. The turbulence rotation is decreased at the barrier, which again demonstrates the braking effect of the DED. The acceleration of rotation by counter neutral beam injection and braking by the DED yields an increase in the velocity shear at $r/a = 0.9$. At the barrier, the level of density fluctuations is constant, the turbulence decorrelation time is increased and the turbulence wavelength is decreased. The evaluation of turbulent diffusion using a random walk model yields the reduction of transport by $\sim$50% within the barrier.

3.3. Transport barriers during OH discharges in TUMAN-3M

The influence of LF magnetohydrodynamic (MHD) activity bursts during ohmic H-mode in the TUMAN-3M tokamak [6] has been studied focusing on the measurements of plasma fluctuation poloidal velocity performed by microwave Doppler reflectometry. During the MHD burst a transient deterioration of improved confinement was observed. As shown in figure 3

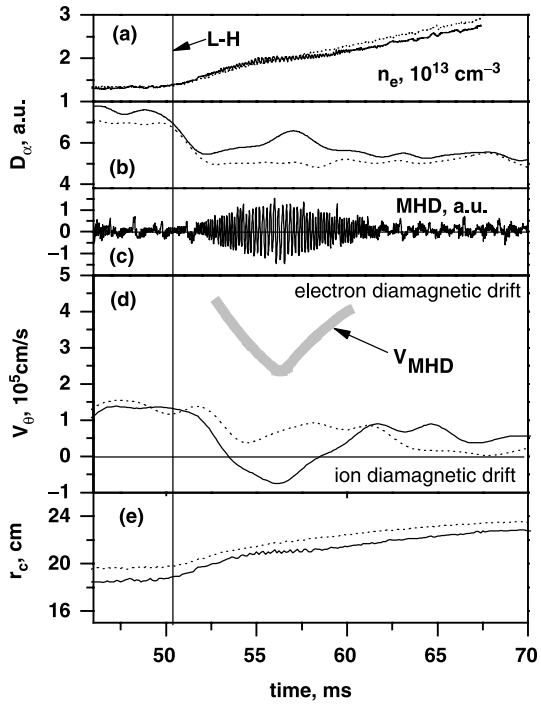

Figure 3. Time evolution of the signals measured in a shot virtually without MHD activity (dotted line) and in a shot with a sharp MHD in TUMAN-3M; (*a*) line averaged plasma density measured along central chord, (*b*) Dα emission intensity, (*c*) magnetic probe signal with MHD burst, (*d*) magnetic island poloidal velocity derived from magnetic probe signal evolution (thick grey curve) and the Doppler velocities, (*e*) cut-off radii (dotted line, microwave frequency 23.5 GHz and solid line, microwave frequency 24.68 GHz).

the plasma fluctuation poloidal rotation observed prior to the MHD burst in the vicinity of the edge transport barrier was in the direction of plasma drift in the negative radial electric field. During the MHD activity the measured poloidal velocity was drastically decreased and even changed its sign. Radial profiles of the poloidal velocity measured in a series of reproducible tokamak shots exhibited the plasma fluctuation rotation in the ion diamagnetic drift direction at the location of the peripheral transport barrier.

The positive E_r perturbation at the plasma edge obviously leads to a transient deterioration of the H-mode transport barrier. On the other hand, the inward propagation of the positive electric field increases the shear of plasma rotation deeper in the core. Such a displacement of the shear pattern to the core region might cause a transport barrier shift towards the inner region of the plasma column.

3.4. Periodic collapse of transport barrier induced by edge biasing in CASTOR

Electrode biasing experiments performed on the tokamak CASTOR ($R_0 = 0.40$ m, $a = 0.085$ m) [21] resulted effectively in inducing improved plasma confinement, characterized by the establishment of an edge transport barrier, featuring steeper density and radial electric field gradients [22]. Above a threshold bias voltage critical gradients are periodically achieved both

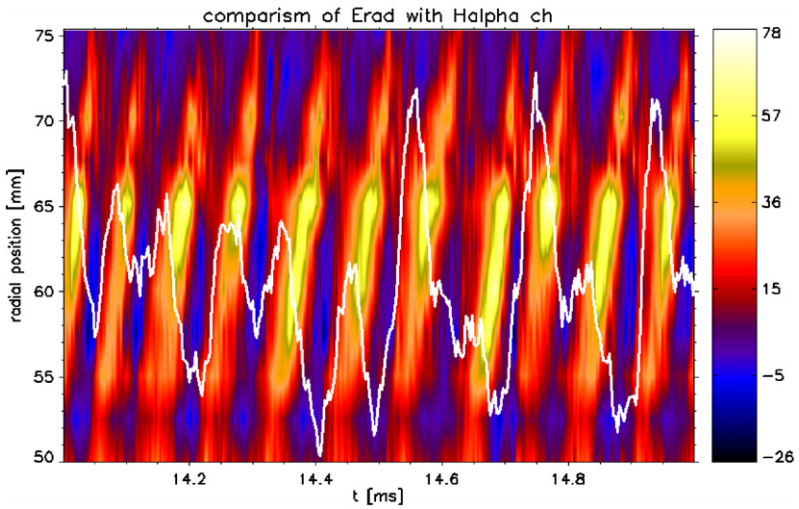

Figure 4. Comparison of the temporal evaluation of the floating potential with the time trace of the H_α line radiation (white curve) in CASTOR.

in floating potential and plasma density, and are followed by a relaxation phase by a frequency of ∼10 kHz.

The high time and spatial resolution electrostatic diagnostics allowed a detailed investigation of relaxation events occurring during the biasing phase. A poloidal array of 96 Langmuir probes [23], 16 magnetic coils and 16 Hall sensors surrounding the full poloidal circumference monitors poloidal profiles of electric field, density and magnetic field with high temporal resolution. A radial array of Langmuir probes measures the radial profiles of floating potential, poloidal electric field and ion saturation current. A Gundestrup probe measures the parallel and perpendicular flows while a segmented tunnel probe measures the electron and ion temperatures. All data are acquired with up to 1 MHz sampling rate.

A biasing voltage of +200 V is applied to a graphite electrode immersed in the edge plasma of the tokamak. During biasing a clear and reproducible transition to improved confinement is routinely observed along with the formation of an edge transport barrier which is characterized by (a) steepening of the time-averaged density gradient, (b) reduction in recycling and (c) substantial improvement of the global particle confinement. A strongly sheared radial electric field is created within the transport barrier followed by an abrupt collapse of the potential and density gradients. Figure 4 shows a detail of the creation and collapse of the transport barrier together with the corresponding evolution of the H_α line radiation. First, a strong transport barrier of width ∼4–5 mm is periodically formed in the proximity of the LCFS, in the range of radii 55–67 mm. Then, it propagates radially towards the wall with a velocity of $\sim 220\,\mathrm{m\,s^{-1}}$. Finally, the barrier collapses, when it is approaching the LCFS, which is located at $r = 67.2$ mm in this particular case. The H_α line starts to decrease, when the strong barrier is formed at 55–60 mm. This can be interpreted as a reduction of convective transport towards the wall and consequently the reduction of recycling. When the barrier collapses, the plasma burst interacts with the walls (or limiter) and the recycling and H_α intensity increase.

The transport barrier is periodically created and relaxes with frequency ∼10 kHz. The maximum radial electric field within the transport barrier is up to $70\,\mathrm{kV\,m^{-1}}$, which causes strong ExB rotation in the poloidal direction. The resulting poloidal velocity (up to $50\,\mathrm{km\,s^{-1}}$)

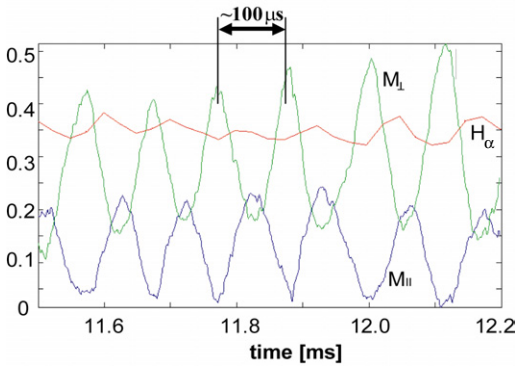

Figure 5. Temporal evolution of the parallel $M_{\|}$ and perpendicular $M_{\perp}$ Mach numbers and of the H_{α} line radiation in CASTOR.

is comparable to the ion sound velocity. Figure 5 presents the temporal evolution of the parallel and perpendicular flows, determined from Gundestrup, robe data [19]. The periodic redistribution of the plasma flow between the parallel and perpendicular directions is observed with characteristic frequency of ∼10 kHz. The breakdown of transport barrier is followed by an increase of the parallel flow along with an increase of the H_{α} radiation due to enhanced influx of neutrals into the plasma, appearing shortly after.

The observed radial propagation of dense structures and fast spikes of electron temperature immediately following the collapse indicates the ejection of hot dense plasma towards the wall. This process is repetitive with a frequency ∼10 kHz throughout the full biasing phase of the discharge. The observed relaxation events are found to be associated with a stream of density radially propagating towards the wall.

The poloidal Langmuir probe array data show that the relaxations are poloidally symmetric with poloidal mode number $m \sim 0$. The spectra of magnetic perturbations measured with a poloidal array of Mirnov coils show in the ohmic phase of the discharge the presence of a magnetic island $m = 3$ at $f = 80$ kHz. During the relaxations, magnetic activity is observed at $f \sim 10$ kHz with a poloidal mode number $m = 0$–1, while the $m = 3$ magnetic island is fully suppressed. This indicates a significant redistribution of the current density profile during the relaxations.

4. Turbulence characteristics

4.1. Geodesic acoustic modes (GAM)

Geodesic acoustic modes (GAM) were investigated on the *T-10 tokamak* using the HIBP, CR and multipin Langmuir probe diagnostics [24]. Regimes with ohmic heating and with on- and off-axis ECRH were studied. It was shown that GAM are mainly potential oscillations, but GAM are pronounced enough in the density fluctuation to be detected by CR, making the latter to an effective tool for further study of zonal flows (ZF)/GAM.

Typically, the power spectrum (figure 6) of the HIBP potential oscillations exhibits a dominating solitary quasi-monochromatic peak. GAM are torsional plasma oscillations with poloidal wave number $m = 0$, a high frequency branch of ZF. The frequency of GAM changes in the region of observation and decreases towards the plasma edge. After ECRH switch-on, the frequency increases, correlating with growth of the electron temperature T_e. The GAM

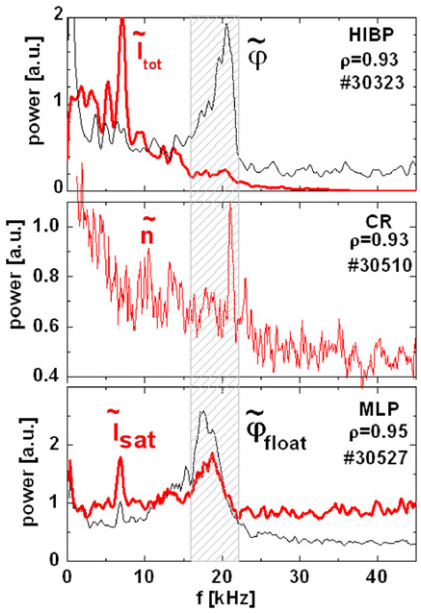

Figure 6. (*Top graph*) Power spectrum of potential oscillations and total beam current (proportional to the plasma density) measured by HIBP in T-10; (*Middle graph*) Spectrum of plasma density oscillations measured by the reflectometer; (*Bottom graph*) Spectra of floating potential and ion saturation current oscillations measured by the Langmuir probe. Parameters of similar shots: $B_T = 2.42$|,T, $Ip = 290$ kA, $q(a) = 2.5$, $n_e = 4 \times 1019\,m^{-3}$.

frequency (see figure 7) depends on the local T_e as: $f_{GAM} \sim c_s/R \sim T_e^{1/2}$ which is consistent with a theoretical scaling for GAM, where c_s is the sound speed within a factor of unity.

Along with the above-mentioned features, predicted for ZF/GAM, some additional characteristics were found on T-10:

- GAM tend to be more excited near low-q magnetic surfaces.
- Along with being mainly electrostatic, GAM also have some magnetic component.
- GAM amplitude has an intermittent character.
- GAM exhibit a density limit.

Characteristics of GAM observed with O-mode CR in OH discharges in the plasma edge of the *TEXTOR tokamak* are similar to those on T-10 [25]. The frequency of the observed mode obeys the theoretically predicted GAM scaling with local temperature and ion mass. The poloidal distribution of the amplitude of the GAM-induced density fluctuations was studied. On the basis of measurements at several poloidal positions a good qualitative agreement with theoretically predicted $\sin\theta$ (or $m = 1$) distribution was found. The phase coherence over about 90° confirms the long-scale nature of the observed density oscillations which is also consistent with the predicted $m = 1$ structure. The level of the oscillations of turbulence rotation related with the GAM is found to be in the range 5–10% of the ambient turbulence rotation, which result in an increase of shearing rate by a factor of ∼5. The resulting shearing rate is comparable to the decorrelation rate of the ambient turbulence. It is shown that the fluctuations in the ambient plasma turbulence level are strongly correlated with those of the oscillations of turbulence rotation due to GAM.

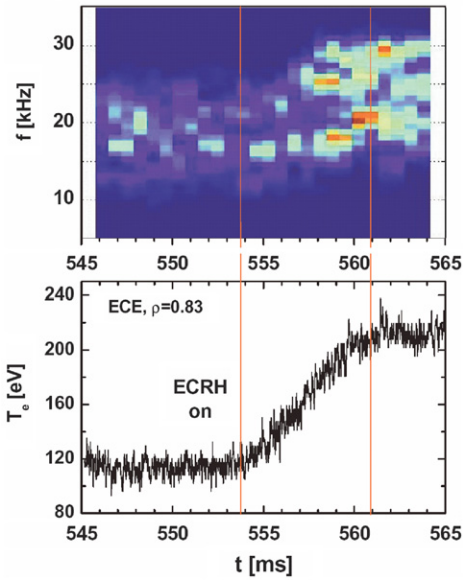

Figure 7. Evolution of spectrum measured at $\rho = 0.83$ during ECRH switch-on in T-10. The frequency of peak increases together with growth of electron temperature.

Doppler reflectometry has recently been employed to detect GAM as oscillations of poloidal velocity in the ASDEX Upgrade tokamak [26]. A similar diagnostic has been used to reveal GAM oscillations in the *TUMAN-3M tokamak* during transition to ohmic H-mode triggered by impulse gas puffing [27]. The oscillations of poloidal velocity in the GAM frequency region were evaluated via the averaging of the Doppler frequency shift spectra. To study an influence of the GAM oscillations on the RMS level of plasma scattering fluctuations cross-correlation spectral analysis has been employed. Quasi-coherent (QC) oscillations of the poloidal velocity in the GAM frequency region between 20 and 40 kHz were observed. The oscillations were detected for cut-off locations near the edge transport barrier occurring during the H-mode. There is no QC oscillation of the poloidal velocity if the cut-off is located in the SOL. The discovered correlation between the plasma fluctuation level and the poloidal velocity oscillation indicates an impact of the GAM oscillations on the plasma turbulence.

4.2. Core turbulence characteristics in T-10

Turbulence characteristics were investigated in detail in OH and ECRH discharges in T-10 using CR, HIBP and Langmuir probe arrays [28]. The OH and ECRH discharges show a distinct transition from the core turbulence, having a complex spectral structure, to the unstructured one at the plasma boundary.

The core turbulence includes the 'broad band' (BB), 'quasi-coherent' (QC) features, arising due to the excitation of rational surfaces with high poloidal m-numbers, 'low frequency' (LF) near zero frequency, and the GAM oscillations at 20–30 kHz. All experimentally measured properties of LF and HF QC are in good agreement with the behaviour of the linear increments of ion temperature gradient/dissipative trapped electron mode (ITG/DTEM) instabilities. Significant local decrease of the turbulence amplitude and coherency was

observed at the edge velocity shear layer and in the core near $q = 1$ radius at 5–15 ms after ECRH switch-off.

Reflectometry at half minor radius shows that long wavelength turbulence is replaced by shorter wavelength turbulence when the density increases up to half of the Greenwald density. The shorter wavelength turbulence is dominant at higher densities. This observation offers the possibility to explain the confinement rise at low and its saturation at higher densities. The second factor, which may influence the confinement, is the strong decrease of the Te/Ti ratio with the density increase which could also lead to the confinement rise.

4.3. Turbulence characteristics in FT-2

The new highly localized UHR BS diagnostics (see section 2.4) capable of determining the small scale turbulence wave number spectra were developed at the FT-2 tokamak ($R_0 = 0.56$ m, $a = 0.08$ m) [7] and provided the following results:

- Two modes are found in the UHR BS spectra under conditions when the threshold for the ETG mode instability [29] is exceeded. The ETG mode is a possible candidate to explain anomalous electron energy transport.
- The first mode has a frequency <1 MHz and radial wave number $25\,\mathrm{cm}^{-1} < q < 150\,\mathrm{cm}^{-1}$, and is localized at the plasma edge and associated with the ITG mode. Its wave number spectrum is quickly decaying in a way similar to that observed on Tore Supra.
- The second mode has a frequency higher than 2 MHz and radial wave number $q > 150\,\mathrm{cm}^{-1}$, and is associated with the ETG mode. Its phase velocity is twice as high and its amplitude is growing towards the centre. In the region of observations its level is comparable to that of the ITG mode but is however much smaller than that of the latter mode at the edge.
- The possibility of the poloidal rotation profile determination with the UHR BS technique is demonstrated.

4.4. Conclusions and outlook

The strong innovation potential of this INTAS project lies in the field of tokamak physics and tools to control plasma turbulence and electric fields, as well as in the field of advanced plasma diagnostics. This project led to an improved understanding of the relation between the global confinement properties of tokamak plasmas and the physics of the electrostatic and magnetic turbulence.

The main goal of the coherent approach was to identify the major physical laws and instabilities ruling the transport in tokamak plasmas in order to incorporate them into theoretical turbulence models as well as in analytical transport models. This is of crucial importance, because the ITER project relies mostly on scaling laws. A thorough understanding can pave new ways towards advanced scenarios and their external control, and hence lead to an optimized construction of next generation tokamaks. Any new ideas on external control of transport barriers by means of magnetic and electrostatic perturbation on the plasma edge can be easily tested since the tokamaks in the project can be relatively easily modified according to new ideas.

The main findings in the field of transport barriers are as follows: (a) The only possibility of organizing a more peaked pressure profile than the self-consistent profile is the establishment of pronounced ITBs; the hypothesis is that it is determined by the density of turbulent cells in the vicinity of low-order rational surfaces. (b) The combination of counter-current neutral

beam injection and DED in TEXTOR can lead to the formation of a transport barrier at the plasma edge. The turbulence rotation is decreased at the barrier due to the braking effect of the DED. (c) LF MHD activity bursts during ohmic H-mode in the TUMAN-3M tokamak lead to a transient deterioration of improved confinement. The poloidal velocity of the fluctuations is drastically decreased and even changed its sign in the ion diamagnetic drift direction at the location of the edge transport barrier. (d) A clear and reproducible transition to a regime with improved particle confinement is routinely observed on the CASTOR tokamak. The steepening of the radial profiles of the plasma density and potential demonstrate the formation of a transport barrier just inside the LCFS. Fast relaxations of the edge profiles, with a frequency $\sim$10 kHz, are observed when the average radial electric field within the barrier exceeds values of about $\sim$20 kV m^{-1}.

The main findings in the field of turbulence characteristics are as follows: (a) GAM have been clearly identified in T-10, TEXTOR and TUMAN-3M using advanced diagnostics. (b) Turbulence characteristics were investigated in detail in OH and ECRH discharges in T-10 using CR, HIBP and Langmuir probe arrays. The OH and ECRH discharges show a distinct transition from the core turbulence, having a complex spectral structure, to the unstructured one at the plasma boundary. (c) Electrostatic fine scale ETG mode turbulence (a possible candidate to explain anomalous electron energy transport in tokamak plasmas have been identified in FT-2 using an experimental tool — correlative UHR.

A new INTAS project has started in October 2006 with the same partners plus four other institutions. This will in addition provide advanced theoretical models and numerical simulations, access to the long pulse tokamak Tore Supra and the availability of advanced magnetic sensors to study magnetic turbulence inside the plasma.

Acknowledgments

The authors are grateful to INTAS (International Association for the promotion of co-operation with scientists from the New Independent States of the former Soviet Union), which supported the research activities in the framework of project INTAS 2001-2056, and for support from RFBR and NWO (grants RFBR 05-012-17016, NSH-2264.2006.2 and NWO-RFBR 047.016.015) and the Flemish Research Foundation FWO.

References

[1] Melnikov A *et al* 2006 *Plasma Phys. Contr. F.* **48** S87, and references therein
[2] World survey of major facilities in controlled fusion 1976 *Nucl. Fusion* Special supplement p 700
[3] Vershkov V A *et al* 2005 *Nucl. Fusion* **45** 203 and references therein
[4] Kraemer-Flecken A *et al* 2004 *Nucl. Fusion* **44** 1143
[5] 2005 *Fusion Sci. Techn.* **47** (special issue on TEXTOR)
[6] Bulanin V V *et al* 2006 *Plasma Phys. Control. Fusion* **48** A101
[7] Gusakov E Z *et al* 2006 *Plasma Phys. Control. Fusion* **48** A371
[8] Gusakov E Z *et al* 2006 *Plasma Phys. Control. Fusion* **46** 1393
[9] Gusakov E Z *et al* 2006 *Plasma Phys. Control. Fusion* **47** 959
[10] Peleman P *et al* 2006 *J. Nucl. Mater.* at press
[11] Tendler M, Van Oost G and Stöckel J 2002 *Comment Modern Phys.* **2** N6, C 203
[12] Dnestrovskij Yu N *et al* 2006 *Nucl. Fusion* **46** 953
[13] Razumova K A *et al* 2004 *Nucl. Fusion* **44** 1067
[14] Razumova K A *et al* 2006 *Plasma Phys. Control. Fusion* **48** 1373
[15] Baranov Yu F *et al* 2004 *Plasma Phys. Control. Fusion* **46** 1181
[16] Waltz R.E *et al* 2006 *Phys. Plasmas* **13** 052301
[17] Brakel R *et al* 2002 *Nucl. Fusion* **42** 903

[18] Finken K H *et al* 1997 *Fusion Eng. Des.* **37** 335
[19] Peleman P *et al* 2006 *Rev. Scient. Instr.* at press
[20] Kraemer-Flecken A *et al* 2006 *Nucl. Fusion* **46** 730
[21] Van Oost G *et al* 2003 *Plasma Phys. Control. Fusion* **45** 621 and references therein
[22] Spolaore M *et al* 2005 *Czech. J. Phys.* **55** 1597
[23] Stockel J *et al* 2005 *Plasma Phys. Control. Fusion* **47** 635
[24] Melnikov A V *et al* 2006 *Plasma Phys. Control. Fusion* **48** S87
[25] Kraemer-Flecken A *et al* 2006 *Phys. Rev. Lett.* 045006
[26] Conway G *et al* 2005 *Plasma Phys. Control. Fusion* **47** 1165
[27] Bulanin VV *et al Proc. 32nd EPS Conf. On Controlled Fusion and Plasma Physics (Tarragona, Spain 2005)* vol 29C 4.051
[28] Vershkov V A *et al* 2005 *Nucl. Fusion* **45** 203
[29] Jenko F *et al* 2001 *Phys. Plasmas* **8** 4096